Journal of Molecular Graphics and Modelling 52 (2014) 36–45

Contents lists available at ScienceDirect

Journal of Molecular Graphics and Modelling

journal homepage: www.elsevier.com/locate/JMGM

# Theoretical prediction of structural, vibrational and NMR parameters of plastic optical fiber (POF) material precursors. Cis and trans perhydro- and perfluoro-2-methylene-4,5-dimethyl-1,3-dioxolanes

Farhod Nozirov [a,**], Teobald Kupka [b,*], Michał Stachów [b]

[a] Department of Physics, 4513 Manhattan College Parkway Riverdale, New York 10471, USA
[b] Faculty of Chemistry, Opole University, 48, Oleska Street, 45-052 Opole, Poland

ARTICLE INFO

*Article history:*
Accepted 17 June 2014
Available online 24 June 2014

*Keywords:*
Perfluoro-2-methylene-4,5-dimethyl-1,3-dioxolane
POF
DFT
GIAO NMR

ABSTRACT

Density functional theory (DFT) prediction of cis and trans perhydro- and perfluoro-2-methylene-4,5-dimethyl-1,3-dioxolanes structure, supported by vibrational analysis and calculation of multinuclear isotropic nuclear magnetic resonance (NMR) shieldings and indirect spin–spin couplings (SSCCs) was performed. The performance of the used methodology was verified on 1,3-dioxolane selected as model compound. The structures of hydrogenated and fluorinated monomers of POF materials were calculated using B3LYP and BLYP density functionals combined with 6-311++G(3df,2pd) basis set. The BLYP/6-311++G(3df,2pd) level of theory was suggested for vibrational analysis. Gauge independent atomic orbitals (GIAO) calculations were applied to distinguish between cis and trans isomers of the title 1,3-dioxolanes. For obtaining both accurate nuclear shieldings and individual spin–spin coupling constants the BHandH/aug-pcJ-2 level of theory was chosen. The protocol used for the calculations nicely showed remarkable differences in vibrational spectra and NMR parameters of cis and trans isomers of the studied 1,3-dioxolane derivatives before and after fluorination.



## 1. Introduction

With the recent advent of information transfer using waveguide techniques, the pursuit for novel POF materials [1–5] is among the forefront topics in material sciences. The properties of these polymer materials are critically dependent on the understanding and controlling monomer structure, properties and their purity [1,2,6–10]. Polymer optical fiber (POF) is produced from monomers yielding amorphous material with relatively high glass transition temperature ($T_g$), low signal loss in the near infrared electromagnetic frequency region (NIR) and high bandwidth [3–5,11]. Such materials are obtained by polymerization of specific monomers containing in their structure fluorine instead of hydrogen, e.g. perfluorinated molecules. The production and separation of perfluorinated monomers instead of typical hydrocarbon monomers is a complex industrial process. Historically, the free radical homopolymerization leading to tetrafluoroethylene was applied by Du Pont in 1937 [12]. On the other hand, perfluorodiene monomers were introduced by Asahi Glass in 1989 [13,14]. Perfluoro-2-methylene-1,3-dioxolane (PMMD or PFMMD) was obtained by DuPont in 1967 [15] and independently by Asahi Glass in 1993 [16]. Due to low efficiency and high costs of the existing production methods of fluorinated polymers there has been a constant search for improvement in this field.

One of the important issues in production of POF materials is qualitative and quantitative characterization of the obtained fluorinated monomers and their radical polymerization products. The one- and two-dimensional multinuclear ($^1$H, $^{13}$C and $^{19}$F) NMR spectroscopy in solution and their numerous variants in the solid state are the methods of choice for characterization of such systems. There appeared several excellent experimental reports on synthesis and NMR characterization of PFMMD monomers and polymers by teams of Liu [3], Okamoto [3,9,10,17] and Rinaldi [1].

On the other hand, theoretical prediction of structure and spectroscopic parameters has been frequently used to support experimental works [18–24]. Despite very accurate (benchmark) results obtained for small molecules with very sophisticated methods including electron correlation (e.g. coupled cluster with single, double and perturbative treatment of triples, CCSD(T) [25–28]) and very large and flexible one-electron basis sets [29–32] there

* Corresponding author. Tel.: +48 665 921 475.
** Corresponding author.
*E-mail addresses:* farhod.nozirov@gmail.com (F. Nozirov), teobaldk@gmail.com, teobaldk@yahoo.com (T. Kupka).

http://dx.doi.org/10.1016/j.jmgm.2014.06.004
1093-3263/

are more affordable and robust methods producing fairly accurate results for larger size molecules [33]. The latter methods are rooted in density functional theory (DFT [34,35]). Prediction of structural parameters (e.g. bond lengths, angles and dihedral angles) is very often performed with efficient hybrid functional B3LYP [36–38]. However, the vibration frequencies in harmonic approximation are lower and closer to experiment using BLYP density functional [37–39] instead of B3LYP. In general, the theoretically predicted harmonic frequencies overestimate the observed values by 3–5% due to the neglect of anharmonicity effect [40–43]. Thus, frequency scaling [40] is a practical way to bring the calculated results to closer agreement with the observed spectral signals. The use of anharmonic model [44–46] is significantly more expensive computationally and the selection of a functional which is capable of producing wavenumbers closer to experiment (e.g. without resorting to anharmonic model) is another option. From our earlier vibrational studies on several small molecules we noticed that BLYP produces results significantly closer to experiment [47–49].

It is well known that the NMR shieldings (and to the less extend the chemical shifts) and indirect spin–spin coupling constants are very sensitive to the density functional type used and the basis set construction [50–55]. Among the basis sets tailored for accurate calculations of nuclear shieldings and spin–spin coupling parameters are systematically improved pcS-n [56] and pcJ-n [57] series of basis sets ($n = 0, 1, 2, 3$ and 4). Apparently, the values of three bond HCCH and FCCF coupling constants could be used as a sensitive parameter for characterization of cis/trans systems [58]. However, earlier studies by Contreras and coworkers [59] pointed out the discrepancy between DFT calculations and experiment for the spin–spin coupling constants (SSCC) involving fluorine nuclei. Thus, in our studies we performed both shielding calculations and SSCC prediction using the BHandH density functional [60]. This density functional was able to predict fairly reliable NMR parameters for $F_2$ and $F_2O$ molecules [61] which are very difficult for theoretical calculations [54].

In our recent study [60] we checked the performance of BHandH [62,63] and VSXC [64] density functionals and very large basis sets for accurate prediction of isotropic nuclear magnetic shieldings and indirect spin–spin coupling constants in 1,1-difluoroethylene and cis- and trans-1,2-difluoroethylenes. The DFT optimized structures of these isomers were similar to geometries obtained at benchmark CCSD(T)/CBS level of theory [65]. In addition, the NMR parameters calculated using these functionals were close to MP2 and coupled cluster values.

In this work we aim at theoretical characterization of cis and trans perhydro- and perfluoro-2-methylene-4,5-dimethyl-1,3-dioxolane [1] structures and prediction of their vibrational and multinuclear NMR spectra. Their simplified structures and atom numbering are shown in Scheme 1. The appropriately chosen molecular modeling protocol for their theoretical characterization will be proposed as a potential tool supporting assignment of IR/Raman and NMR spectra of various PFMMD monomers.

The performance of the used methodology (density functional type and basis set) will be verified on two 1,3-dioxolanes [66–68] as model compounds (see Scheme 2).

The 1,3-dioxolanes were selected as simplified models of PFMMD for several reasons. First, they contain $sp^3$ hybridized carbon atoms and also two hydrogen/fluorine atoms in different arrangement in space in respect to the C—C bond (cis and trans) in five membered heterocyclic molecule. The 1,3-dioxolane ring non-planarity was studied some time ago [69]. In our study we will report the calculated ring twist angle [69]. Besides, their structure, as well as vibrational and NMR spectroscopic parameters are well characterized both by experimental and theoretical methods [69]. Finally, the structure of 1,3-dioxolane formed by a five-membered ring with two oxygen atoms closely resembles the ring of PFMMD.

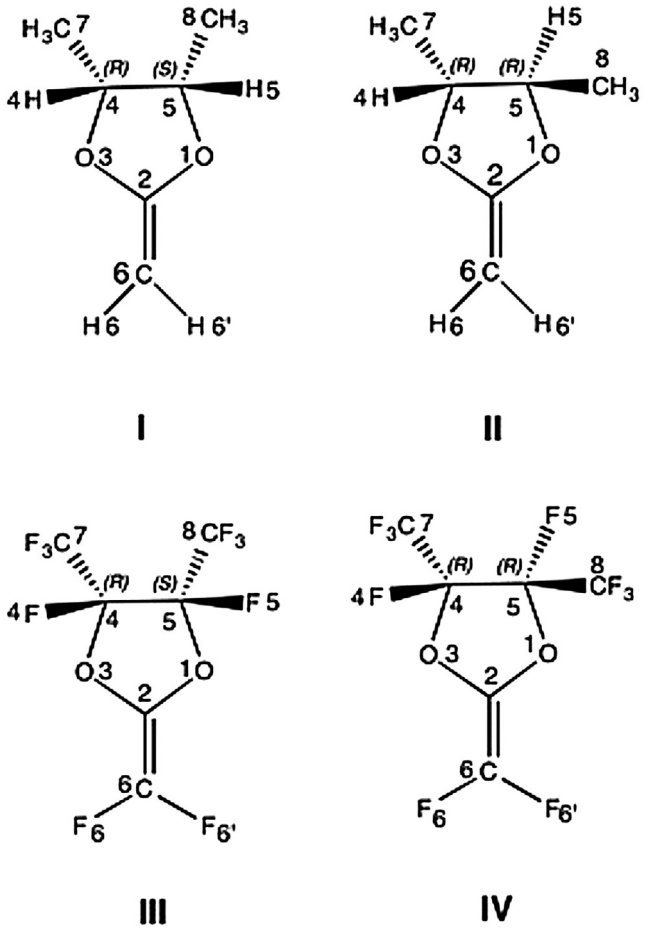


**Scheme 1.** Two configurational isomers (H-cis, **I**, (*4R,5S*)-4,5-dimethyl-2-methylene-1,3-dioxolane and H-trans, **II**, (*4R,5R*)-4,5-dimethyl-2-methylene-1,3-dioxolane) and their perfluorinated analogs (F-cis, **III**, (*4R,5S*)-4,5-trifluorodimethyl-2-difluoromethylene-1,3-dioxolane and F-trans, **IV**, (*4R,5R*)-4,5-trifluorodimethyl-2-difluoromethylene-1,3-dioxolane).

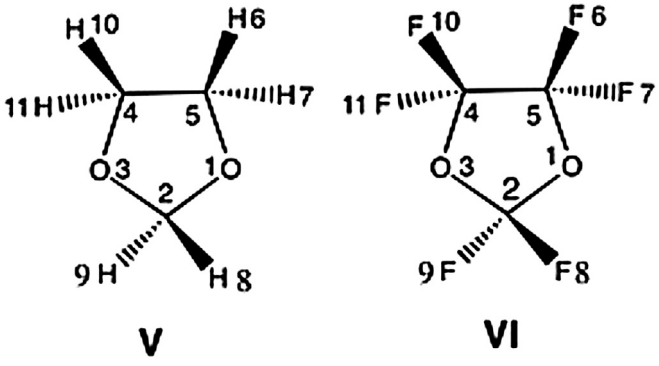


**Scheme 2.** Structures of (**V**) 1,3-dioxolane and (**VI**) perfluoro-1,3-dioxolane.

## 2. Theoretical methodology

All calculations were performed using Gausian 09 program package [63]. Pople type basis set 6-311++G(3df, 2pd) from Gaussian internal library was used. Jensen's type pc-n [70,71], pcS-n [56] and pcJ-n [57] basis sets were downloaded from EMSL [72]. All the studied molecules (**I–VI** in Schemes 1–2) are nonplanar and rapid conformational changes result in averaging their parameters at normal conditions. 1,3-dioxolane (**V**) [66–68] and its perfluorinated derivative (**VI**) were selected to assess the accuracy of the used

**Table 1**
Comparison of averaged structural parameters of 1,3-dioxolane ($\mathbf{C_3O_2H_6}$) and fluorinated 1,3-dioxolane ($\mathbf{C_3O_2F_6}$), calculated using 6-311++G(3df,2pd) basis set with earlier reports [67,68] and experiment [66].

| | $C_3O_2H_6$ | | | | | | | $C_3O_2F_6$ | |
|---|---|---|---|---|---|---|---|---|---|
| | B3LYP | BLYP | MP2 | MP2[a] | MP2[b] | Exp.[c] | Exp.[d] | B3LYP | BLYP |
| Bond [Å] | | | | | | | | | |
| C2O | 1.4108 | 1.4268 | 1.4083 | 1.407 | 1.424 | 1.423 | 1.430 | 1.3853 | 1.4034 |
| C4O | 1.4271 | 1.4471 | 1.4242 | 1.424 | 1.442 | | 1.415 | 1.3795 | 1.3971 |
| C4C5 | 1.5340 | 1.5531 | 1.5259 | 1.524 | 1.536 | 1.542 | 1.530 | 1.5708 | 1.5862 |
| C2X | 1.0943 | 1.1013 | 1.0914 | | 1.103 | 1.106 | | 1.3302 | 1.3496 |
| C4X | 1.0913 | 1.0976 | 1.0898 | | 1.100 | 1.106 | | 1.3333 | 1.3526 |
| C5X | 1.0911 | 1.0974 | 1.0892 | | 1.101 | 1.106 | | 1.3333 | 1.3526 |
| RMS[c] | 0.013 | 0.008 | 0.016 | 0.017 | 0.005 | | | | |
| RMS[d] | 0.013 | 0.023 | 0.014 | 0.015 | 0.016 | | | | |
| Angle [°] | | | | | | | | | |
| OC2O | 106.97 | 106.67 | 107.07 | 106.9 | 107.02 | 108.7 | 107.6 | 109.17 | 109.57 |
| C2OC | 106.11 | 105.31 | 104.95 | 106.8 | | 105.8 | 106.8 | 110.69 | 110.29 |
| OCC | 103.45 | 104.08 | 102.98 | 103.8 | 103.35 | 101 | 102.1 | 104.11 | 104.36 |
| XCX | 109.32 | 109.39 | 109.87 | | | | | 107.99 | 107.78 |
| XC2X | 110.69 | 111.10 | 111.18 | | | | | 107.46 | 107.32 |
| RMS[c] | 1.7 | 2.1 | 1.6 | | | | | | |
| RMS[d] | 0.9 | 1.5 | 1.2 | | | | | | |
| Dihedral [°] | | | | | | | | | |
| C5C4O3C2 | 36.12 | 32.98 | 40.26 | 26 | 26.34 | 41.8 | 38.4 | 9.13 | 8.71 |
| Dev.[c] | −5.7 | −8.8 | −1.5 | | | | | | |
| Dev.[d] | −2.3 | −5.4 | 1.9 | | | | | | |

[a] MP2(FULL)/6-311++G(2df,2p) results from Ref. [67].
[b] MP2/aug-cc-pVDZ results from Ref. [68].
[c] from Ref. [66].
[d] experimental values cited in Ref. [67] were taken from Ref. [66] (these authors followed a procedure from Ref. [78]).

methodology. Their structures and atom numbering are shown in Scheme 2. These model molecules were fully optimized using B3LYP, BLYP and MP2 methods combined with 6-311++G(3df,2pd) basis set. Selection of such large and flexible basis set, augmented with diffuse functions was necessary for fairly accurate prediction of their structure. Thus, this level of calculations should produce results similar to those, obtained with Dunning's type aug-cc-pVDZ or even aug-cc-pVTZ basis sets. However, the obtained parameters are still far from the complete basis set limit while the computations are being significantly cheaper than using aug-cc-pVTZ [73,74] or pc-3 [70] basis sets. The subsequent vibrational analysis verified the presence of minimum energy structures (lack of imaginary frequencies).

Next, the fully optimized B3LYP/6-311++G(3df,2pd) structures of I–IV were used as input for GIAO [75,76] NMR calculations of nuclear shieldings and estimation of SSCC values using BHandH density functional combined with aug-pcJ-2 basis set. The aug-pcJ-2 belongs to the Jensen's family of basis sets [57] which produce SSCC values regularly converging toward CBS limit [29,53,77]. It also yields very accurate nuclear isotropic shieldings [52]. In the subsequent text, the "X" letter was used for H or F atoms. Note, that due to molecular symmetry in the remaining text we will omit some atom numbering in the calculated parameter listings. Finally, the quality of theoretical (predicted) data was expressed as deviation from experiment ($x_{calc} - x_{exp}$) and in a form of root-mean-square (RMS) calculated for n similar parameters as: $RMS = \sqrt{[((x_1 - x_{exp})^2 + \cdots + (x_n - x_{exp})^2)/n]}$.

## 3. Results and discussion

In the first step of our study we performed full geometry optimization followed by vibration analysis of 1,3-dioxolanes (see Scheme 2 for atom numbering). The selected B3LYP, BLYP and MP2 bond lengths and bond angles were calculated with 6-311++G(3df,2pd) basis sets and compared with few available experimental values and high level theoretical parameters from the literature [66–68] (see Table 1). It was pleasing to notice that the RMS deviations of B3LYP, BLYP and MP2 calculated bond lengths from two available experiments (0.013, 0.008, 0.016 and 0.013, 0.023, 0.014 Å) were fairly small and comparable to those, reported earlier (0.005–0.017 Å). Thus, the applied density functionals approached the performance of the earlier reported MP2 theory [67,68]. The structural parameters of 1,3-dioxolane predicted with B3LYP density functional were marginally closer to experimental values than the results obtained with BLYP (see Table 1). Similar performance of these density functionals in prediction of 1,1- and 1,2-difluoroethylene isomers structure was recently observed [60] (in particular, the B3LYP and BLYP calculated RMS values of CF distances and angles were 0.004 vs. 0.022 Å and 0.3 vs. 0.5°). Looking at individual bond lengths, the theoretically predicted C2O bond was consistently shorter than C4O by about 0.02 Å, both in our calculations, and in earlier MP2 studies [67,68]. However, these bonds were fairly accurate (within ±0.01 to ±0.02 Å from experimental values [66]).

The theoretically predicted harmonic B3LYP, BLYP and anharmonic B3LYP wavenumbers corresponding to six highest frequency modes for 1,3-dioxolane were gathered in Table 2 and compared with the best literature numbers and observed frequencies [67,68,79]. By analogy, the six highest frequencies of perfluorinated 1,3-dioxolane are also included. For these modes are observed the largest difference between harmonic frequencies and experiment (about 100 $cm^{-1}$), as well as anharmonic B3LYP results. As expected, the anharmonicity of the remaining 1,3-dioxolane modes for wavenumbers below 1500 $cm^{-1}$ are significantly smaller and are within a few $cm^{-1}$. For brevity, all the vibrational frequencies are gathered in Table S1 in the supplementary material.

Interestingly, the deviation between theoretical harmonic wavenumbers of 1,3-dioxolane, calculated with B3LYP density functional and the observed values [68] is about two times higher than for BLYP density functional (RMS of about 53 vs. 34 $cm^{-1}$) and the significantly more expensive VPT2 anharmonic procedure combined with B3LYP produces the best agreement (RMS = 28 $cm^{-1}$). In case of 1,1-, cis- and trans-difluoroethylenes the same order of RMS values (B3LYP > BLYP > B3LYP (anharm)) was observed [60]. For example, in case of 1,1-difluoroethylene [60], the following RMS were obtained with B3LYP(harm), BLYP (harm) and

**Table 2**
Comparison of six highest frequency harmonic and anharmonic vibrations of 1,3-dioxolane ($\mathbf{C_3O_2H_6}$) calculated using 6-311++G(3df,2pd) basis set with experiment and earlier reports [67,68,79]. For comparison are shown the highest frequency wavenumbers predicted for fluorinated 1,3-dioxolane ($\mathbf{C_3O_2F_6}$).

| Mode | $C_3O_2H_6$ | | | | | | | $C_3O_2F_6$ | |
|---|---|---|---|---|---|---|---|---|---|
| | B3LYP (harm) | B3LYP (anharm) | BLYP (harm) | MP2 (harm) | Lit.[a] | Lit.[b] | Exp.[c] | B3LYP (harm) | BLYP (harm) |
| 1 | 3115.5 | 2978.4 | 3035.7 | 3182.8 | 3184 | 3206 | 3018 | 1382.50 | 1292.66 |
| 2 | 3090.5 | 2917.3 | 3022.8 | 3164.9 | 3175 | 3192 | 2996 | 1266.04 | 1182.88 |
| 3 | 3070.4 | 2944.4 | 2994.5 | 3147.3 | 3150 | 3170 | 2975 | 1231.65 | 1146.12 |
| 4 | 3031.2 | 2863 | 2951.5 | 3086.9 | 3088 | 3113 | 2904 | 1230.88 | 1142.43 |
| 5 | 2994.3 | 2844.7 | 2918.9 | 3052.1 | 3054 | 3078 | 2886 | 1209.77 | 1117.18 |
| 6 | 2945.7 | 2837.6 | 2849.2 | 3014.6 | 3017 | 3035 | 2852 | 1193.01 | 1109.6 |
| RMS[d] | 52.9 | 28.2 | 34.1 | 85.6 | 82.6 | 100.3 | – | – | – |

[a] From Ref. [68].
[b] MP2(full)/6-311++G(2df,2p) results from Ref. [67].
[c] In Ar matrix at 10 K and ratio 1:12, Ref. [68].
[d] RMS deviation from values observed in Ar matrix at 10 K and ratio 1:12, Ref. [68].

B3LYP(anharm): 53, 36 and 18 $cm^{-1}$. It was also very disappointing to notice a very significant discrepancy between MP2 (harm) calculated 1,3-dioxolane wavenumbers and experiment (RMS = 86 $cm^{-1}$). However, the latter result was similar or slightly better to earlier reported deviations (RMS of 83 and 100 $cm^{-1}$ [67,68]). Thus, the results from Table 2 point out at BLYP density functional in combination with 6-311++G(3df,2pd) basis set as a pragmatic choice for calculating reliable fundamental frequencies of 1,3-dioxolane. The B3LYP and BLYP calculated harmonic wavenumbers of perfluoro-1,3-dioxolane are spread in significantly smaller frequency range (20–1400 $cm^{-1}$). It is evident from Table 2 that the latter density functional should reproduce closer experimental data and could be used for assigning bands in future experimental IR and Raman studies of similar compounds (to the best of our knowledge no experimental data for the perfluoro derivative are available yet).

On the other hand, the reader should be aware that exceptionally good performance of BLYP in reproducing experimental wavenumbers, as compared to B3LYP (and many other functionals) could be traced to fortuitous error cancelation. For example, as result of improvement of coupled cluster theory level and basis set completeness, the calculated parameters somehow systematically approach the experimental values. However, in contrary to coupled cluster methods, this is not true for numerous density functionals, designed to well reproduce only selected experimental data (the lack of an ideal density functional is an old issue).

In the next step we performed full optimization of the cis and trans isomers for both perhydrogenated and perfluorogenated molecules I–IV, shown in Scheme 1, using B3LYP and BLYP density functionals and 6-311++G(3df,2pd) basis set. The selected structural results (bonds and angles) of the four molecules are shown in Table 3. Additionally, we used pc-2 basis set to check whether a better basis set produces structures and frequencies significantly different. These results are very similar and therefore will not be discussed here. However, for completeness, we included them in separate tables in the supplementary material. As result of different atomic radii, the C—H bond is shorter than the corresponding C—F bond (it increases from 1.09 to about 1.33–1.39 Å). This also results in stronger steric effect of $CF_3$ groups in comparison to $CH_3$. As result, the adjacent C—$CF_3$ bond is also elongated (from 1.51 to 1.57 Å). Fluorination also makes the five-membered ring more planar (dihedral angle decreases from about 15° in case of hydrogenated molecules to about 10° degree).

It is apparent from Tables 4 and S3 (Supplementary material) that the B3LYP calculated harmonic frequencies are about 40 $cm^{-1}$ higher (on average) than those, obtained with BLYP density functional. Judging from the results obtained recently for difluoroethylenes [60], the BLYP functional produces harmonic vibrations closer to experimental values than traditional B3LYP density functional. In other words, we could expect that the BLYP results in Table 4 are closer to experiment (see also the conclusions in earlier reports [47–49,60]).

Interestingly, the corresponding IR and Raman spectra of perfluorinated molecules are simpler (see Figs. 1–4) and the Raman active C=C stretch is very intense. Replacement of H atoms by F is observed as disappearance of symmetric and asymmetric C—H stretch signals near 3000 $cm^{-1}$. Besides, the C—F stretch range, typical for many other vibrations in non-fluorinated compounds (between 800 and 1300 $cm^{-1}$) is not so pronounced in the spectral patterns. In Fig. 1A and B are shown BLYP/6-311++G(3df,2pd) calculated IR

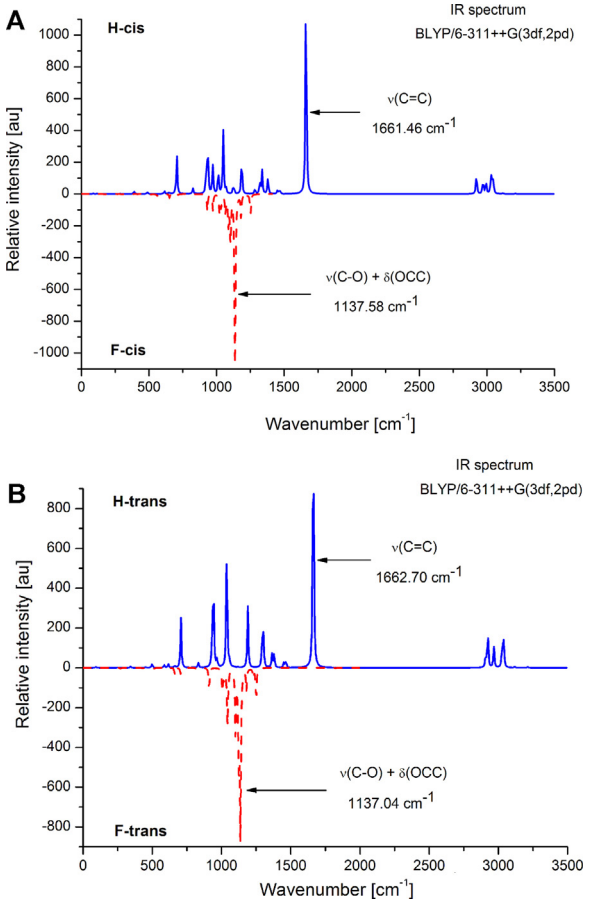


**Fig. 1.** BLYP/6-311++G(3df,2pd) calculated IR spectrum of (A) cis and (B) trans forms of H- and F-monomers (see Scheme 1).

**Table 3**
The selected structural results (bonds and angles) of molecules I–IV, calculated with B3LYP and BLYP density functionals combined with 6-311++G(3df,2pd) basis set (X is H or F atom, respectively).

| | H-cis | | H-trans | | F-cis | | F-trans | |
|---|---|---|---|---|---|---|---|---|
| | B3LYP | BLYP | B3LYP | BLYP | B3LYP | BLYP | B3LYP | BLYP |
| **Bond** [Å] | | | | | | | | |
| O1C5 | 1.4404 | 1.4621 | 1.4392 | 1.4609 | 1.3793 | 1.3949 | 1.3825 | 1.3987 |
| O3C4 | 1.4423 | 1.4642 | 1.4392 | 1.4609 | 1.3954 | 1.4125 | 1.3825 | 1.3987 |
| O1C2 | 1.3600 | 1.3760 | 1.3610 | 1.3775 | 1.3723 | 1.3878 | 1.3708 | 1.3866 |
| O3C2 | 1.3620 | 1.3788 | 1.3610 | 1.3775 | 1.3684 | 1.3835 | 1.3708 | 1.3866 |
| C4C5 | 1.5372 | 1.5484 | 1.5295 | 1.5401 | 1.5850 | 1.6048 | 1.5681 | 1.5829 |
| C2C6 | 1.3283 | 1.3390 | 1.3281 | 1.3388 | 1.3208 | 1.3334 | 1.3207 | 1.3333 |
| C6X6 | 1.0765 | 1.0826 | 1.0765 | 1.0826 | 1.3165 | 1.3336 | 1.3163 | 1.3333 |
| C6X6′ | 1.0765 | 1.0826 | 1.0765 | 1.0826 | 1.3165 | 1.3336 | 1.3163 | 1.3333 |
| C4C7 | 1.5192 | 1.5298 | 1.5115 | 1.5220 | 1.5580 | 1.5736 | 1.5562 | 1.5715 |
| C5C8 | 1.5114 | 1.5219 | 1.5115 | 1.5220 | 1.5522 | 1.5672 | 1.5562 | 1.5715 |
| C7X | 1.0896 | 1.0959 | 1.0898 | 1.0971 | 1.3328 | 1.3521 | 1.3318 | 1.3510 |
| C8X | 1.0892 | 1.0956 | 1.0898 | 1.0971 | 1.3318 | 1.3510 | 1.3318 | 1.3510 |
| C4X4 | 1.0895 | 1.0961 | 1.0960 | 1.1023 | 1.3463 | 1.3676 | 1.3635 | 1.3873 |
| C5X5 | 1.0951 | 1.1016 | 1.0960 | 1.1023 | 1.3464 | 1.3868 | 1.3635 | 1.3873 |
| **Angle** [°] | | | | | | | | |
| O3C2O1 | 110.42 | 110.68 | 110.51 | 110.76 | 111.21 | 111.46 | 111.04 | 111.27 |
| C5O1C2 | 108.05 | 107.69 | 108.50 | 108.14 | 107.82 | 107.69 | 108.78 | 108.45 |
| C4O3C2 | 108.68 | 108.36 | 108.50 | 108.14 | 109.44 | 109.32 | 108.78 | 108.45 |
| C5C4O3 | 101.09 | 101.20 | 102.00 | 102.11 | 102.26 | 102.52 | 103.20 | 103.24 |
| C4C5O1 | 101.71 | 101.84 | 102.00 | 102.11 | 103.40 | 103.60 | 103.20 | 103.24 |
| **Twist**[a] | 15.32 | 15.48 | −14.17 | −14.40 | 11.06 | 10.14 | −11.15 | −11.54 |

[a] half of O1C5C4O3 dihedral angle.

spectra of cis and trans isomers of hydrogenated and perfluorinated molecules I–IV. As expected, fluorination leads to significant simplification of IR spectra of both isomers. First of all, several bands of relatively weak intensity which are due to CH stretch modes near 3000 $cm^{-1}$ and the strongest single band in the spectrum (C=C stretch mode at about 1660 $cm^{-1}$) disappear completely. Secondly, the main part of spectrum, between 700 and 1400 $cm^{-1}$, changes to more crowded signals (and in narrower region of spectrum) for the corresponding fluorinated compounds. Besides, the most intense signal in these spectra (at about 1140 $cm^{-1}$) is due to a more complex vibrational mode, including both stretching of O1—C5 (and O3—C4) bonds and deformation of O1—C5—C8 (and O3—C4—C7) bond angles. It is also important to notice that fluorination leads to disappearance of C=C stretching mode (its IR intensity is very low).

Comparing the IR (Fig. 1) and Raman (Fig. 2) spectra of the studied compounds, it is possible to distinguish between H-cis and F-cis isomers, as well as between H-trans and F-trans on the basis of the differences in their spectra. However, only minor differences in their IR and Raman spectra do not allow for an easy discrimination between H-cis and H-trans or F-cis and F-trans.

Similarly to IR spectra, the Raman active signals reveal the presence of C—H groups in compounds **I**–**II**. In fact, the stretch C—H signals are the most intense ones in the BLYP/6-311++G(3df,2pd) calculated Raman spectra of both H-cis and H-trans compounds. A significantly weaker single peak due to C=C stretch (at about 1160 $cm^{-1}$) is also visible in these spectra and the remaining peaks in the spectral range from 500 to 1500 $cm^{-1}$ appear very weak in H-molecules and much stronger in case of perfluorinated compounds. In contrary to IR spectra (Fig. 1) of perfluorinated compounds, the Raman spectroscopy should reveal the most intense, single band at about 1820 $cm^{-1}$ due to C=C stretch in both fluorinated isomers (Fig. 2, bottom spectra).

The B3LYP/6-311++G(3df,2pd) and BLYP/6-311++G(3df,2pd) calculated selected (the highest frequencies) harmonic vibrations of H- and F-forms of both molecules (see **I–IV** in Scheme 1) are gathered in Table 4.

The results presented in Figs. 1 and 2 indicate a fairly direct and easy way of discrimination between hydrogenated and fluorinated compounds **I** vs. **III** and **II** vs. **IV**. However, the situation gets much more difficult in case of IR spectra of cis and trans isomers of compounds **I** and **II** (Fig. 3), as well as in Raman spectra of compounds **III** and **IV** (Fig. 4). In fact, only fairly small differences

**Table 4**
Selected highest frequency harmonic vibrations (in $cm^{-1}$) of the four molecules (see **I–IV in** Scheme 1) calculated with B3LYP and BLYP density functionals combined with 6-311++G(3df,2pd) basis set.

| **No.** | H-cis | | H-trans | | F-cis | | F-trans | |
|---|---|---|---|---|---|---|---|---|
| | B3LYP | BLYP | B3LYP | BLYP | B3LYP | BLYP | B3LYP | BLYP |
| 1 | 3285.89 | 3210.40 | 3286.38 | 3210.91 | 1916.89 | 1822.78 | 1917.47 | 1823.11 |
| 2 | 3189.80 | 3117.93 | 3190.38 | 3118.59 | 1342.92 | 1252.45 | 1340.85 | 1250.49 |
| 3 | 3123.37 | 3047.76 | 3114.20 | 3038.87 | 1332.24 | 1247.84 | 1333.91 | 1247.69 |
| 4 | 3114.47 | 3040.66 | 3113.21 | 3037.88 | 1308.06 | 1216.28 | 1318.19 | 1229.31 |
| 5 | 3107.64 | 3031.60 | 3104.44 | 3028.95 | 1260.22 | 1181.08 | 1259.50 | 1180.03 |
| 6 | 3104.72 | 3028.12 | 3102.51 | 3027.13 | 1243.89 | 1152.92 | 1246.09 | 1158.37 |
| 7 | 3071.44 | 2993.13 | 3038.06 | 2967.54 | 1227.83 | 1137.58 | 1224.13 | 1137.04 |
| 8 | 3043.46 | 2972.48 | 3036.79 | 2966.26 | 1214.56 | 1133.49 | 1218.29 | 1125.91 |
| 9 | 3037.20 | 2966.09 | 3001.92 | 2923.50 | 1193.67 | 1103.07 | 1200.85 | 1119.46 |
| 10 | 3000.81 | 2921.92 | 2986.62 | 2907.89 | 1189.39 | 1099.16 | 1191.92 | 1100.63 |
| 11 | 1730.89 | 1661.46 | 1732.14 | 1662.70 | 1173.04 | 1086.56 | 1155.89 | 1081.54 |

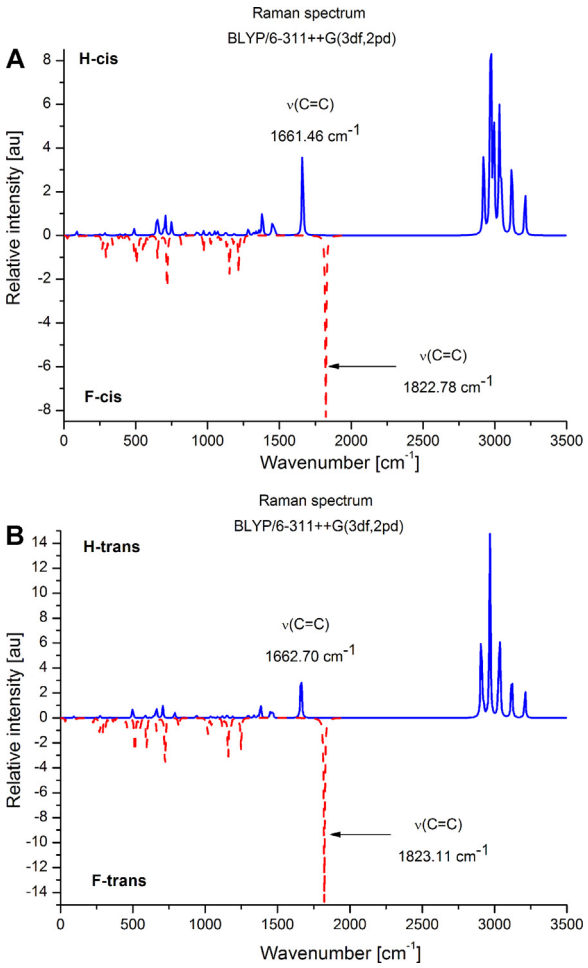


**Fig. 2.** BLYP/6-311++G(3df,2pd) calculated Raman spectra of (A) cis and (B) trans forms of H- and F-monomers (see Scheme 1).

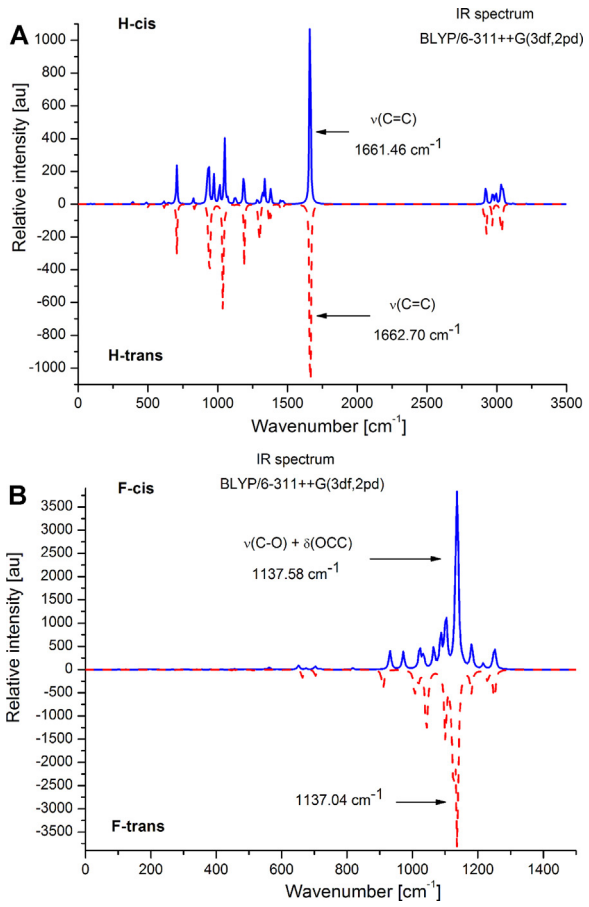


**Fig. 3.** BLYP/6-311++G(3df,2pd) calculated IR spectrum of cis- and trans-forms of (A) H- and (B) F-monomers I–IV (see Scheme 1).

between cis and trans forms could be noticed from these spectra. Thus, comparing the overall spectral patterns it is apparent that trans isomers of both H- and F-compounds show somehow simpler (and less crowded) spectral patterns with better separated lines than due to the presence of the corresponding cis-systems. However, the most intense peaks in both types of spectra are practically predicted at the same wavenumbers (see Figs. 3 and 4). Therefore, vibrational spectroscopy could serve as a tool to easily distinguish the presence of fluorinated systems **III** and **IV** among **I** and **II** but the analysis of cis/trans systems, e.g. **I** vs. **II** or **III** vs. **IV**, is more challenging.

The BHandH/aug-pcJ-2 GIAO NMR calculated isotropic nuclear magnetic shieldings and the averaged SSCC values at B3LYP/6-311++G(3df,2pd) geometries of 1,3-dioxolane (**$C_3O_2H_6$**) and fluorinated 1,3-dioxolane (**$C_3O_2F_6$**) are shown in Table 5.

Experimental NMR spectra of 1,3-dioxolane in CDCl3 were reported long time ago [80]: the signals due to hydrogen atoms at C2 and C4,5 were observed at 4.57 and 3.57 ppm relative to internal TMS. Using TMS shielding value of 31.62 ppm (see Ref. [24]) this can be converted to observed proton chemical shieldings 27.05 and 28.05 ppm, respectively. Significantly more accurate chemical shifts were reported in Ref. [81].

By replacing H atoms with fluorine large changes are observed in NMR parameters of 1,3-dioxolanes (Table 5). The most pronounced decrease of nuclear shielding is observed for oxygen (from 265 to 137 ppm). Besides, the isotropic nuclear shieldings of both carbon atoms also increase (from 33 to 60 ppm). The two $^1$H NMR signals

**Table 5**
Comparison of average nuclear isotropic shieldings[a] [b] (σ) and indirect spin–spin coupling constants ($^nJ_{AB}$) of 1,3-dioxolane (**$C_3O_2H_6$**) and fluorinated 1,3-dioxolane (**$C_3O_2F_6$**).

| | $C_3O_2H_6$ | | $C_3O_2F_6$ |
|---|---|---|---|
| Nuclei | σ [ppm] | | |
| | DFT | Exp. | |
| O | 265.1803 | 262.653[c] | 136.7432 |
| C2 | 86.221 | 93.01[d] | 53.4112 |
| C4 | 118.9983 | 123.51[d] | 58.1945 |
| (C2)X | 26.4183 | 26.718[e] | 241.3667 |
| (C4)X | 27.4723 | 27.643[e] | 273.8112 |
| SSCC | | $^nJ_{AB}$ [Hz] | |
| $^1J_{CX}$ | | | |
| at C2 | 163.87 | 165[f] | −284.29 |
| at C4 | 147.1 | 149[f] | −300.01 |
| $^1J_{CC}$ | 34.37 | | 84.88 |
| $^2J_{CC}$ | −0.92 | | 5.62 |
| $^2J_{XX}$ | | | |
| at C2 | −1.04 | | 57.55 |
| at C4 | −8.63 | | 128.12 |
| $^3J_{XXcis}$ | 8.08 | | −9.21 |
| $^3J_{XXtras}$ | 11.03 | | 8.08 |

[a] BHandH/aug-pcJ-2 GIAO NMR and subsequent indirect spin–spin coupling constants calculations on B3LYP structures optimized with 6-311++G(3df,2pd) basis set.
[b] X is H or F atom (for atom numbering see Scheme 2).
[c] Recalculated from experimental value of $\delta = 33.0$ ppm in Ref. [82], using water as reference (calculated at the same level of theory, $\sigma = 331.7527$ ppm).
[d] From experimental $^{13}$C spectra[81] relative to TMS ($\sigma = 188.15$ ppm).
[e] From experimental $^1$H spectra[81] relative to TMS ($\sigma = 31.30$ ppm).
[f] From Ref. [83].

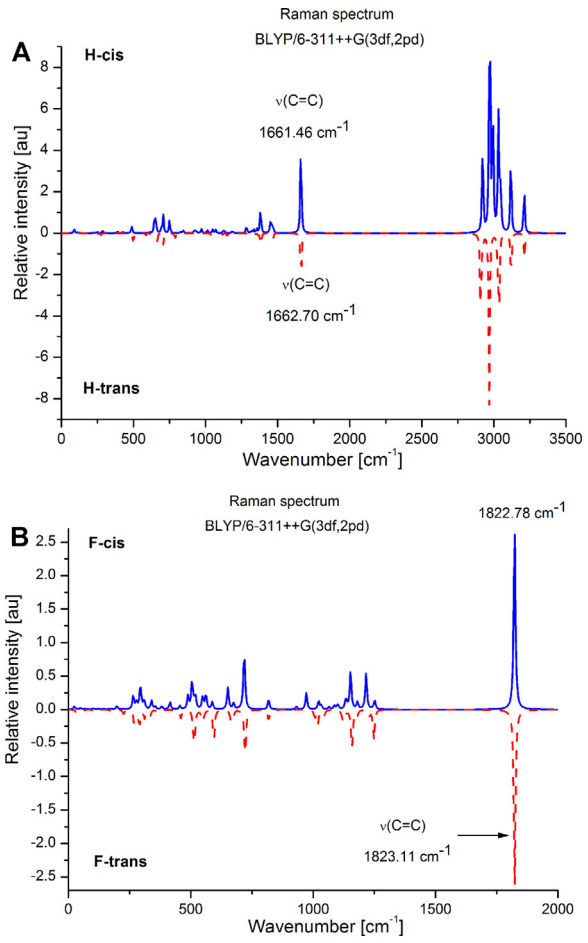


**Fig. 4.** BLYP/6-311++G(3df,2pd) calculated Raman spectrum of cis- and trans-forms of (A) H- and (B) F-monomers I–IV (see Scheme 1).

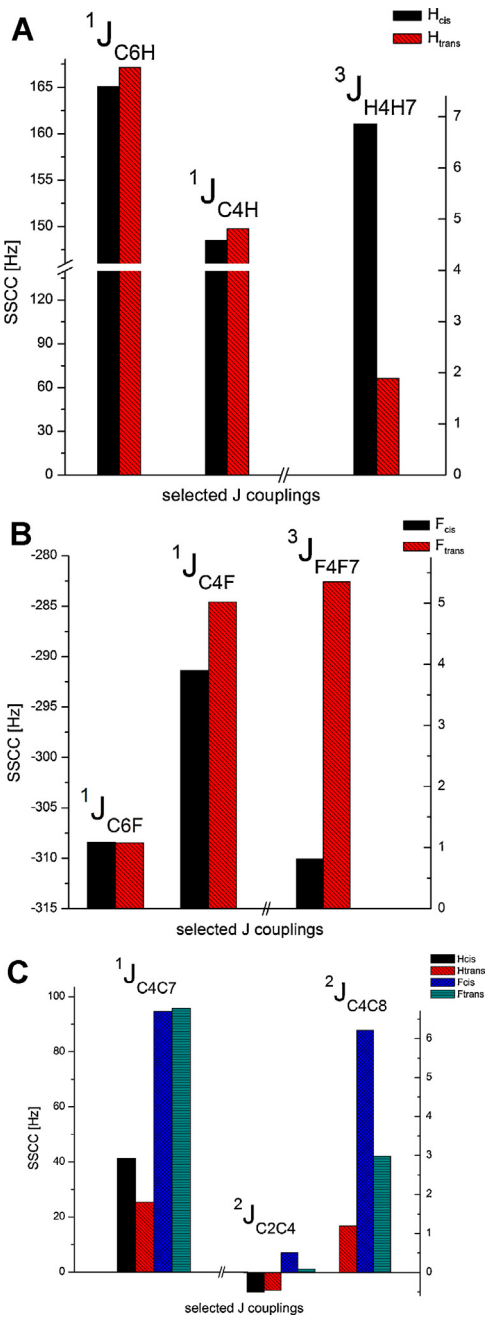


**Fig. 5.** Selected BHandH/aug-pcJ-2 calculated coupling constants in I–IV molecules: (A) $^{1}J_{CH}$ and $^{3}J_{HH}$, (B) $^{1}J_{CF}$ and $^{3}J_{FF}$ and (C) $^{1}J_{CC}$ and $^{3}J_{CC}$.

due to protons attached to C2 and C4 differ by about 1 ppm and upon replacement by fluorine the corresponding $^{19}F$ signals differ by about 33 ppm (the order of signals is unchanged).

Replacement of hydrogen atoms by fluorine in 1,3-dioxolane results in very large changes in the corresponding indirect spin–spin coupling constants (Table 5). The magnitude of two $^{1}J_{CH}$ couplings (164 and 147 Hz) is about two times larger and of opposite sign in $^{1}J_{CF}$ (−284 and −300 Hz). The $^{1}J_{CC}$ increases about three times (from 34 to 85 Hz) in fluorinated 1,3-dioxolane. The geminal $^{2}J_{HH}$ (−1 and −8.6 Hz) is much smaller than for $^{2}J_{FF}$ (58 and 128 Hz). However, the result for $^{2}J_{FF}$ should be considered only as semi-quantitative. In case of 1,1-difluoroethylene this parameter was underestimated by about 45 Hz [60]. Interestingly, the $^{3}J_{XX}$ for protonated and fluorinated compounds follow the same order (cis < trans). In addition, the difference (trans–cis) is 3 and 17 Hz for X=H and F, respectively. It is important to mention that at this level of theory the $^{3}J_{FF}$ in 1,2-difluoroethylenes was significantly more accurately predicted than $^{2}J_{FF}$ [60].

A very similar picture of NMR shieldings and spin–spin couplings (Table 6) is observed for molecules I–IV (see Scheme 1). Therefore, a different spacial arrangement of substituents in H-cis and H-trans molecules seems to be responsive for different nuclear isotropic shieldings of individual atoms. For example, the calculated shieldings of C2 (7.65 and 4.25 ppm), C4 (106.28 and 102,61 ppm), C5 (107.00 and 102.61 ppm) and O3 (177.04 and 183.98 ppm) in cis and trans isomers differ by 3–8 ppm. The isotropic shieldings of some atoms in cis and trans isomers of fluorinated molecules also differ. This is clearly visible for shielding of C2 (37.16 and 35.13 ppm), C5 (71.78 and 69.24 ppm) and O3 (206.86 and 196.74 ppm) atoms.

The indirect spin–spin coupling constant values predicted for molecules **I–IV** are also sensitive to cis or trans position of substituents. For example, the calculated $^{1}J(CH)$ in the cis and trans isomers is 165.09 and 167.13 Hz. In case of $^{3}J(HH)$ at C4 and C5 carbons these values are 6.86 and 1.89 Hz. For the corresponding perfluorinated cis and trans isomers significant differences between calculated $^{1}J(CF)$ at C4 and $^{3}J(FF)$ at C4 and C5 atoms are predicted (−291.39 vs. −284.59 Hz and 0.81 vs. 5.35 Hz). This is also illustrated in Fig. 5 showing the differences between selected two and three-bond carbon-carbon spin–spin constants for these molecules. Thus, both nuclear shieldings and indirect spin–spin coupling constants are ideal spectroscopic parameters enabling determination of cis and trans isomers of **I–IV** molecules.

**Table 6**
Comparison of averaged nuclear isotropic shieldings[a] [b] ($\sigma$) and indirect spin–spin coupling constants ($^nJ_{AB}$) of perhydrogenated and perfluorinated monomers I–IV.

| **Nuclei** | (**I**) H-cis | (**II**) H-trans | (**III**) F-cis | (**IV**) F-trans |
|---|---|---|---|---|
| | $\sigma$ [ppm] | | | |
| C2 | 7.6538 | 4.2487 | 37.1459 | 35.1324 |
| C4 | 106.2842 | 102.6076 | 69.2017 | 69.2382 |
| C5 | 107.0016 | 102.6076 | 71.7845 | 69.2382 |
| C6 | 126.9854 | 127.0163 | 28.3412 | 28.4815 |
| C7 | 173.1727 | 166.6268 | 57.9571 | 58.5086 |
| C8 | 173.5656 | 166.6268 | 58.5852 | 58.5086 |
| X4 | 26.9769 | 27.1950 | 327.3902 | 319.2707 |
| X5 | 26.9436 | 27.1950 | 315.2632 | 319.2707 |
| X6 | 27.8154 | 27.7985 | 316.2131 | 317.1234 |
| X6′ | 27.8014 | 27.7985 | 318.5574 | 317.1234 |
| (C7)$\underline{X_3}$ | 30.2636 | 30.1069 | 268.3127 | 266.2179 |
| (C8)$\underline{X_3}$ | 30.11003 | 30.1069 | 266.0699 | 266.2179 |
| O1 | 186.1425 | 183.9813 | 192.2067 | 196.7386 |
| O3 | 177.0414 | 183.9813 | 206.8558 | 196.7386 |
| **SSCC** | | $^nJ_{AB}$ **[Hz]** | | |
| $^1J_{CX}$ (C6) | 165.085 | 167.125 | −308.422 | −308.464 |
| $^1J_{CX}$ (C4,5) | 148.521 | 149.753 | −291.385 | −284.592 |
| $^1J_{CC}$ (C4,5) | 36.983 | 36.223 | 53.647 | 57.353 |
| $^1J_{CC}$ (C4,5-C7,8) | 41.261 | 40.322 | 94.617 | 95.775 |
| $^2J_{CC}$ (C2-C4,5) | −0.506 | −0.464 | 0.504 | 0.083 |
| $^2J_{CC}$ (C4,5-C8,7) | 0.001 | 1.191 | 6.216 | 2.980 |
| $^2J_{XX'}$ (C6) | −4.176 | −4.005 | 101.775 | 102.401 |
| $^2J_{XX'}$ (C7,8) | −14.026 | −13.828 | 120.777 | 119.381 |
| $^3J_{XX}$ (C4,5) | 6.858 | 1.889 | 0.811 | 5.348 |
| $^1J_{CX}$ (C7) | 126.667 | 126.444 | −312.299 | −313.441 |
| $^1J_{CX}$ (C8) | 126.486 | 126.444 | −314.497 | −313.441 |

[a] BHandH/aug-pcJ-2 GIAO NMR and subsequent indirect spin–spin coupling constants calculations on B3LYP/pc-2 structures.
[b] X is H or F atom (for atom numbering see Scheme 2).

## 4. Conclusions

B3LYP/6-311++G(3df,2pd) and BLYP/6-311++G(3df,2pd) calculated structures of cis and trans perhydro- and perfluoro-2-methylene-4,5-dimethyl-1,3-dioxolanes were reported and the harmonic vibrations calculated at BLYP/6-311++G(3df,2pd) level of theory proposed as more accurate. The obtained results were critically compared to those, obtained for 1,3-dioxolane, selected as model compound and earlier theoretical and experimental reports.

GIAO NMR multinuclear isotropic nuclear magnetic shieldings were calculated using BHandH/aug-cc-pcJ-2 level of theory. The BHandH/aug-cc-pcJ-2 calculations were also used to calculate accurate indirect spin–spin couplings in molecules containing fluorine.

The obtained structural, vibrational and NMR data for cis and trans perhydro- and perfluoro-2-methylene-4,5-dimethyl-1,3-dioxolanes at the proposed composite level of theory could serve to support future more accurate analysis of experimental IR/Raman and NMR spectra of fluorinated monomers used to produce plastic organic fiber (POF) materials.

## Acknowledgments

F. N. is grateful for the VA Montgomery GI bill, VA education benefit from the US Department of Veteran Affairs. Michał Stachów is recipient of a Ph.D. fellowship from a project funded by the European Social Fund Stypendia doktoranckie-inwestycja w kadrę naukową województwa opolskiego. T. Kupka was supported by the Faculty of Chemistry, University of Opole [grant number 8/WCH/2014-S]. The calculation facilities and software in the Supercomputing and Networking Center ACK CYFRONET AGH in Krakow and calculation facilities and software at the Supercomputing and Networking Center in Wrocław are also acknowledged.

## Appendix A. Supplementary data

Supplementary data associated with this article can be found, in the online version, at http://dx.doi.org/10.1016/j.jmgm.2014.06.004.

## References

[1] B. Zhang, L. Li, F. Mikeš, Y. Koike, Y. Okamoto, P.L. Rinaldi, Multidimensional NMR characterization of perfluorinated monomer and its precursors, J. Fluorine Chem. 147 (2013) 40–48.
[2] J. Scheirs, Modern Fluoropolymers, John Wiley and Sons, Chichester, 1997.
[3] W. Liu, Y. Koike, Y. Okamoto, Synthesis and radical polymerization of perfluoro-2-methylene-1,3-dioxolanes, Macromolecules 38 (2005) 9466–9473.
[4] T. Ishigure, S. Tanaka, E. Kobayashi, Y. Koike, Accurate refractive index profiling in a graded-index plastic optical fiber exceeding gigabit transmission rates, J. Lightwave Technol. 20 (2002) 1449–1456.
[5] T. Ishigure, Y. Koike, J.W. Fleming, Optimum index profile of the perfluorinated polymer-based GI polymer optical fiber and its dispersion properties, J. Lightwave Technol. 18 (2000) 178–184.
[6] P.R. Resnick, Polymers of fluorinated dioxoles. DuPont ed., US Patents, USA, 1976, Vol. US3978030 A.
[7] E.N. Squire, Optical fibers comprising cores clad with amorphous copolymers of perfluoro-2,2-dimethyl-1,3-dioxole. DuPont Ed., USA, vol. US4530569, 1985.
[8] M. Nakamura, I. Kaneko, K. Charu, G. Kojima, M. Matsuo, S. Samejima, et al. US Patent 4.897.457 (30 January 1990).
[9] K. Koike, F. Mikeš, H. Zhang, Y. Koike, Y. Okamoto, Synthesis and characterization of copolymers of perfluoro(2-methylene-4,5-dimethyl-1,3-dioxolane) and perfluoro(2-methylene-1,3-dioxolane), J. Fluorine Chem. 156 (2013) 198–202.
[10] F. Mikeš, J. Baldrian, H. Teng, Y. Koike, Y. Okamoto, Characterization and properties of semicrystalline and amorphous perfluoropolymer: poly(perfluoro-2-methylene-1,3-dioxolane), Polym. Adv. Technol. 22 (2011) 1272–1277.
[11] T. Ishigure, M. Sato, A. Kondo, Y. Koike, High-bandwidth graded-index polymer optical fiber with high-temperature stability, J. Lightwave Technol. 20 (2002) 1443–1448.
[12] S.V. Gangal, Tetrafluoroethylene polymers, in: H.F. Mark, N.M. Bikales, N.M. Overberger, G. Menges (Eds.), Encyclopedia of Polymer Science and Engineering, Vol. 16, Willey/Interscience, New York, 1989, pp. 577–642.
[13] M.H. Hung, P.R. Resnick, B.E. Smart, W.H. Buck, Fluorinated plastics, amorphous, in: J.C. Salamone (Ed.), Polymeric Materials Encyclopedia, CRC Press, Boca Raton, FL, 1996, pp. 2466–2476.

[14] M. Nakamura, N. Sugiyama, Y. Etoh, K. Aosaki, J. Endo, Development of perfluoro transparent resins obtained by radical cyclopolymerization for leading-edge electronic and optical applications, Nippon Kagaku Kaishi. 12 (2001) 659–668.
[15] S. Selman, E.N. Squire, Perfluoro(2-methylene-4-methyl-1,3-dioxolane) and polymers thereof. DuPont Ed., USA, vol. US3308107 A, 1967.
[16] O. Kazuya, M. Hidenobu, Fluorinated compound and fluorinated polymer. Japan, vol. JP05-339255, 1993.
[17] F. Mikeš, Y. Yang, I. Teraoka, T. Ishigure, Y. Koike, Y. Okamoto, Synthesis and characterization of an amorphous perfluoropolymer: poly(perfluoro-2-methylene-4-methyl-1,3-dioxolane), Macromolecules 38 (2005) 4237–4245.
[18] K. Jackowski, M. Wilczek, M. Pecul, J. Sadlej, Nuclear pin coupling of 1,2-13C-enriched acetylene in gaseous mixtures with xenon and carbon dioxide, J. Phys. Chem. A. 104 (2000) 5955–5958.
[19] P. Jain, T. Bally, P.R. Rablen, Calculating Accurate Proton Chemical Shifts of Organic Molecules with Density Functional Methods and Modest Basis Sets, J. Chem Theor. Comp. 74 (2009) 4017–4023.
[20] J. Kaski, P. Lantto, J. Vaara, J. Jokisaari, Experimental and theoretical ab initio study of the $^{13}C$–$^{13}C$ spin coupling and $^{1}H$ and $^{13}C$ shielding tensors in ethane, ethene, and ethyne, J. Am. Chem. Soc. 120 (1998) 3993–4005.
[21] J. Kongstead, K. Aidas, K.V. Mikkelsen, S.P.A. Sauer, On the accuracy of density functional theory to predict shifts in nuclear magnetic resonance shielding constants due to hydrogen bonding, J. Chem. Theory Comp. 4 (2008) 267–277.
[22] T. Kupka, H.-M. Lin, L. Stobinski, C.-H. Chen, W.-J. Liou, R. Wrzalik, Z. Flisak, Experimental and theoretical studies on corals I. Toward understanding the origin of color.in precious red corals from Raman and IR spectroscopies and DFT calculations, J. Raman Spectrosc. 41 (2010) 651–658.
[23] T. Kupka, Complete basis set B3LYP NMR calculations of CDCl3 solvent's water fine spectral details, Magn. Reson. Chem. 46 (2008) 851–858.
[24] D. Flaig, M. Maurer, Hanni, K. Braunger, L. Kick, M. Thubauville, Ch. Ochsenfeld, Benchmarking hydrogen and carbon NMR chemical shifts at HF DFT, and MP2 levels, J. Chem Theory Comp. 10 (2014) 572–578.
[25] R.J. Bartlett, Modern Electronic Structure Theory. River Edge, NJ, World Scientific, 1995.
[26] R.J. Bartlett, G.D. Purvis III, Many-body perturbation-theory, coupled-pair many-electron theory, and importance of quadruple excitations for correlation problem, Int. J. Quantum Chem. 14 (1978) 561–581.
[27] J. Noga, R.J. Bartlett, The full CCSDT model for molecular electronic structure, J. Chem. Phys. 86 (1987) 7041–7050.
[28] T. Hrenar, H.-J. Werner, G. Rauhut, Accurate calculation of anharmonic vibrational frequencies of medium sized molecules using local coupled cluster methods, J. Chem. Phys. 126 (13) (2007) 134108.
[29] D. Feller, Application of systematic sequence of wave functions to the water dimer, J. Chem. Phys. 96 (1992) 6104–6114.
[30] D. Feller, The role of databases in support of computational chemistry calculations, J. Comp. Chem. 17 (1996) 1571–1586.
[31] D. Feller, Benchmarks of improved complete basis set extrapolation schemes designed for standard CCSD(T) atomization energies, J. Chem. Phys. 138 (2013) 074103–74109.
[32] D. Feller, K.A. Peterson, An examination of intrinsic errors in electronic structure methods using the environmental molecular sciences laboratory computational results database and the Gaussian-2 set, J. Chem. Phys. 108 (1998) 154–176.
[33] D.M. Reid, R. Kobayashi, M.A. Collins, Systematic study of locally dense basis sets for NMR shielding constants, J. Chem. Theory Comp. 10 (2014) 146–152.
[34] W. Kohn, L.J. Sham, Self-consistent equations including exchange and correlation effects, Phys. Rev. 140 (1965) A1133–A1138.
[35] J.K. Labanowski, J.W. Anzelm, Density Functional Methods in Chemistry, New York, Springer-Verlag, 1991.
[36] A.D. Becke, Density-functional thermochemistry. III. The role of exact exchange, J. Chem. Phys. 98 (1993) 5648–5652.
[37] C. Lee, W. Yang, R.G. Parr, Development of the Colle–Salvetti correlation-energy formula into a functional of the electron density, Phys. Rev. B 37 (1988) 785–789.
[38] B. Miehlich, A. Savin, H. Stoll, H. Preuss, Results obtained with the correlation-energy density functionals of Becke and Lee, Yang and Parr, Chem. Phys. Lett. 157 (1989) 200–206.
[39] A.D. Becke, Density-functional exchange-energy approximation with correct asymptotic behavior, Phys. Rev. A. 38 (1988) 3098–3100.
[40] A.P. Scott, L. Radom, Harmonic vibrational frequencies: an evaluation of Hartree–Fock, Møller–Plesset, quadratic configuration interaction, density functional theory, and semiempirical scale factors, J. Phys. Chem. 100 (1996) 16502–16513.
[41] J.B. Foresman, A. Frisch, Exploring Chemistry with Electronic Structure Methods, second ed, Gaussian Inc., Pittsburg, PA, 1996.
[42] W.J. Hehre, L. Radom, Schleyer P. v.R., J.A. Pople, Ab Initio Molecular Orbital Theory, New York, Wiley, 1986.
[43] R. Burcl, N.C. Handy, S. Carter, Vibrational spectra of furan, pyrrole, and thiophene from a density functional theory anharmonic force field, Spectrochim. Acta A. Mol. Biomol. Spectrosc. 59 (2003) 1881–1893.
[44] D.A. Clabo Jr., W.D. Allen, R.B. Remington, Y. Yamaguchi, H.F. Schaefer III, A systematic study of molecular vibrational anharmonicity and vibration-rotation interaction by self-consistent-field higher-derivative methods. Asymmetric top molecules, Chem. Phys. 123 (1988) 187–239.
[45] O. Christiansen, Vibrational structure theory: new vibrational wave function methods for calculation of anharmonic vibrational energies and vibrational contributions to molecular properties, Phys. Chem. Chem. Phys. 9 (2007) 2942–2953.
[46] V. Barone, Anharmonic vibrational properties by a fully automated second-order. Perturbative approach, J. Chem. Phys. 122 (2005) 014108–14110.
[47] A. Buczek, T. Kupka, M.A. Broda, Extrapolation of water and formaldehyde harmonic and anharmonic frequencies to the B3LYP/CBS limit using polarization consistent basis sets, J. Mol. Model. 17 (2011) 2029–2040.
[48] A. Buczek, T. Kupka, M.A. Broda, Estimation of formamide harmonic and anharmonic modes in the Kohn–Sham limit using the polarization consistent basis sets, J. Mol. Model. 17 (2011) 2265–2274.
[49] A. Buczek, T. Kupka, S.P.A. Sauer, M.A. Broda, Estimating the carbonyl anharmonic vibrational frequency from affordable harmonic frequency calculations, J. Mol. Model. 18 (2012) 2471–2478.
[50] T. Helgaker, M. Jaszuński, K. Ruud, Ab initio methods for the calculation of NMR shielding and indirect spin–spin coupling constants, Chem. Rev. 99 (1999) 293–352.
[51] T. Helgaker, M. Jaszuński, M. Pecul, The quantum-chemical calculation of NMR indirect spin–spin coupling constants, Prog. Nucl. Magn. Reson. 53 (2008) 249–268.
[52] T. Kupka, M. Stachów, M. Nieradka, J. Kaminsky, T. Pluta, Convergence of nuclear magnetic shieldings in the Kohn–Sham limit for several small molecules, J. Chem. Theory Comp. 6 (2010) 1580–1589.
[53] T. Kupka, M. Nieradka, M. Stachów, T. Pluta, P. Nowak, H. Kjear, J. Kongsted Kaminsky, Basis set convergence of indirect spin–spin coupling constants in the Kohn–Sham limit for several small molecules, J. Phys. Chem. A. 116 (2012) 3728–3738.
[54] M.E. Harding, M. Lenhart, A.A. Auer, J. Gauss, Quantitative prediction of gas-phase $^{19}F$ nuclear magnetic shielding constants, J. Chem. Phys. (2008), art. no.244111.
[55] A.M. Teale, O.B. Lutnas, T. Helgaker, D.J. Tozer, J. Gauss, Benchmarking density-functional theory calculations of NMR shielding constants and spin-rotation constants using accurate coupled-cluster calculations, J. Chem. Phys. 138 (2013) 24111–24121.
[56] F. Jensen, Basis set convergence of nuclear magnetic shielding constants calculated by density functional methods, J. Chem. Theory Comp. 4 (2008) 719–727.
[57] F. Jensen, The basis set convergence of spin–spin coupling constants calculated by density functional methods, J. Chem. Theory Comp. 2 (2006) 1360–1369.
[58] M. Karplus, Contact electron-spin coupling of nuclear magnetic moments, J. Chem. Phys. 30 (1959) 11–15.
[59] V. Barone, P.F. Provasi, J.E. Peralta, J.P. Snyder, S.P.A. Sauer, R. Contreras, DFT substituent effects on scalar $^{2}J(^{19}F, ^{19}F)$ and $^{3}J(^{19}F, ^{19}F)$ NMR couplings: a comparison of SOPPA and DFT methods, J. Phys. Chem. A. 107 (2003) 4748–4754.
[60] F. Nozirov, T. Kupka, M. Stachów, Theoretical prediction of nuclear magnetic shieldings and indirect spin–spin coupling constants in 1,1-, cis- and trans-1,2-difluoroethylenes, J. Chem. Phys. 140 (2014), art. no. 144303.
[61] T. Kupka, Convergence of $H_2O$, $H_2$, HF, $F_2$ and $F_2O$ nuclear magnetic shielding constants and indirect nuclear spin–spin coupling constants (SSCCs) using segmented contracted basis sets XZP, polarization-consistent pcS-n and pcJ-n basis sets and BHandH hybrid density functional, Magn. Reson. Chem. 47 (2009) 959–970.
[62] A.D. Becke, A new mixing of Hartree–Fock and local density-functional theories, J. Chem. Phys. 98 (1993) 1372–1377.
[63] M.J. Frisch, G.W. Trucks, H.B. Schlegel, G.E. Scuseria, M.A. Robb, et al., Gaussian 09 Revision D.01, Gaussian, Inc., Wallingford, CT, 2009.
[64] T. Van Voorhis, G.E. Scuseria, A newer form for the exchange-correlation energy functional, J. Chem. Phys. 109 (1998) 400–410.
[65] D. Feller, N.C. Craig, P. Groner, D.C. McKean, Ab initio coupled cluster determination of the equilibrium structures of cis- and trans-1,2-difluoroethylene and 1,1-difluoroethylene, J. Phys. Chem. A 115 (2011) 94–98.
[66] Q. Shen, T.L. Mathers, T. Raeker, R.L. Hilderbrandt, Electron diffraction investigation of pseudorotation in 1,3-dioxolanes, J. Am. Chem. Soc. 108 (1986) 6888–6893.
[67] J. Makarewicz, T.-K. Ha, Ab initio study of the pseudorotation in 1,3-dioxolane, J. Mol. Struct. 599 (2001) 271–278.
[68] V. Mohacek-Grošev, K. Furic, H. Ivankovic, Observed bands in Raman and infrared spectra of 1,3-dioxolane and their assignments, Vibr. Spectrosc. 64 (2013) 101–107.
[69] A. Vila, R.A. Mosquera, On the non-planarity of 1,3-dioxole and 1,3-dioxolane, Chem. Phys. Lett. 488 (2010) 17–21.
[70] F. Jensen, Polarization consistent basis sets: principles, J. Chem. Phys. 115 (2001) 9113–9125.
[71] F. Jensen, Polarization consistent basis sets. II. Estimating the Kohn–Sham basis set limit, J. Chem. Phys. 116 (2002) 7372–7379.
[72] K.L. Schuchardt, B.T. Didier, T. Elsethagen, L. Sun, V. Gurumoorthi, J. Chase, et al., Basis set exchange: a community database for computational sciences, J. Chem. Inf. Model. 47 (2007) 1045–1052 http://bse.pnl.gov/bse/portal
[73] T.H. Dunning Jr., Gaussian basis sets for use in correlated molecular calculations I. The atoms boron through neon and hydrogen, J. Chem. Phys. 90 (1989) 1007–1023.
[74] R.A. Kendall, T.H. Dunning Jr., R.J. Harrison, J. Chem. Phys. 96 (1992) 6796–6806.
[75] R. Ditchfield, Mol. Phys. 27 (1974) 789–807.
[76] K. Wolinski, J.F. Hinton, P. Pulay, J. Am. Chem. Soc. 112 (1990) 8251–8260.

[77] S. Scheiner, Extrapolation to the complete basis set limit for binding energies of noncovalent interactions, Comput. Theoret. Chem. 998 (2012) 9–13.
[78] G. Gundersen, K. Hedberg, Molecular structure of thionyltetrafluoride, $SOF_4$, J. Chem. Phys. 51 (1969) 2500–2507.
[79] S.A. Barker, E.J. Bourne, R.M. Pinkard, D.H. Whiffen, Spectra of acetals. Part I. The infrared and Raman spectra of 1:3-dioxolan, J. Chem. Soc. (1959) 802–806.
[80] E. Caspi, T.A. Wittstruck, D.M. Piatak, The N.M.R. spectra of heterocyclic compounds. I. The spectra of 1,4-dioxanes, 1,3-dioxolanes, and 1,4;5,8-naphthodioxane, J. Org. Chem. 27 (1962) 3183–3189.
[81] SDBC, see at http://sdbs.db.aist.go.jp/sdbs/cgi-bin/direct_frame_top.cgi
[82] D.W. Boykin, $^{17}$O NMR Spectroscopy in Organic Chemistry, CRC, Boca Raton, FL, 1991.
[83] J. Stothers, Organic Chemistry, Academic Press, London, 1972.